Proceedings of the 39th IAHR World Congress
19-24 June 2022
Granada, Spain
DOI number

Tidal Array Spatial Optimisation combining Shallow Water Equations and wake superposition modelling

Connor Jordan[(1)], Davor Dundovic[(2)], Anastasia Fragkou[(1)], Georgios Deskos[(3)], Daniel Coles[(4)], Matthew D. Piggott[(2)] and Athanasios Angeloudis[(1)]

[(1)] School of Engineering, Institute for Infrastructure & Environment, University of Edinburgh, Edinburgh, UK
A.Angeloudis@ed.ac.uk

[(2)] Department of Earth Science and Engineering, Imperial College London, London, UK
M.D.Piggott@imperial.ac.uk

[(3)] National Wind Technology Center, National Renewable Energy Laboratory, Golden, Colorado, USA,
Georgios.Deskos@nrel.gov

[(4)] School of Engineering, Computing and Mathematics, University of Plymouth, Plymouth, UK
Daniel.Coles@plymouth.ac.uk

Abstract

Tidal array optimisation is a multifaceted problem that aims at the improvement of an array design's performance, including its overall power yield. Benefits include reductions in investment uncertainty, thus supporting the tidal stream energy industry to reach its potential. Considering the complex, high-energy tidal hydrodynamics at proposed sites, defining an optimal array layout is challenging and remains an active research area. Existing optimisation methodologies can be either computationally untenable or restrictively simplified for practical cases. We present an optimisation approach that combines an analytical-based wake model, *FLORIS*, with a coastal ocean hydrodynamics model, *Thetis*. The approach is first demonstrated through idealised steady and transient flow cases to highlight hydrodynamics structures that are overlooked, including spatial complexity, tidal asymmetry, and the practical exploitation of blockage effects.. We thus explore the use of analytical wake superposition in combination with the use of simple heuristic techniques to achieve turbine array optimisation at a fraction of the computational cost of alternative methods. Towards this objective, we designed a custom condition-based placement algorithm. The algorithm is applied to the Pentland Firth, including a case of 24 turbines that follow a power curve constrained by a rated speed of ~3.0 m/s. This case study serves to demonstrate device-specific implications whilst also considering the temporal variability of the tide. Overall, this turbine layout optimisation process is able to deliver an array design that is 12% more productive on average than a staggered layout. Performance was quantified through assessment of the optimised layout using a shallow water equation model which more correctly represents turbines through discrete momentum sink terms.

Keywords: Tidal arrays; Shallow water equations; Tidal turbines; Coastal hydrodynamics; Optimisation

1. INTRODUCTION

The tidal stream energy industry is perceived as a reliable renewable energy source and is expected to play a role in decarbonisation efforts at certain coastal regions around the world (Neill et al., 2022). Within UK waters it was recently reported that the practical resource estimate of 34 TWh/year could correspond to 11% of the current annual electricity demand (Coles et al., 2021). Securing this level of contribution is subject to the economic competitiveness of tidal stream array projects, as they expand from the current pilot schemes of a few turbines to form large tidal arrays comprising tens or even hundreds of devices. In the latter case, array layout optimisation will play a crucial role to minimise the interaction among turbines (Funke et al., 2014) and their surrounding environment (Zhang et al., 2022).

Establishing the optimal array layout becomes computationally intensive when interlinked with the hydrodynamics as it presents a partial differential equation (PDE) constrained optimisation problem; recent progress on this front has been reviewed by Piggott et al. (2021). Specifically, there are several studies in the literature that engage in the exploration of array configurations by conducting large numbers of (often 2-D) hydrodynamic simulations with different layouts and turbine tunings; these are notably time and memory intensive, even for idealised settings (Divett et al., 2016). A more sophisticated approach to address the layout optimisation problem has been proposed that uses gradient-based algorithms and adjoint methods to efficiently calculate the objective function gradient, leading to significant reductions in the number of evaluations required (Funke et al., 2014). In this case, adjoint or gradient-based optimisation remains computationally intensive as demonstrated by examples in the literature, which are largely constrained to

idealised and semi-idealised cases. In other approaches that have contributed in this area that consider the hydrodynamics variation over the array (e.g. Phoenix and Nash, 2019) the optimisation framework structure (e.g. mesh constraints or technology parameterisation) is characterised by key trade-offs between computational time and the resolution used to characterise hydrodynamics processes such as wake evolution.

This study seeks to consider the layout optimisation problem, through the overarching goal of an array optimisation strategy that is computationally efficient and extensible to the multi-objective optimisation settings sought thereafter. Additionally, it must be reliable, accurate and acknowledge important hydrodynamic factors and turbine characteristics that affect the optimal array design and performance. This paper demonstrates an optimisation approach which retrofits an analytical wake model designed for wind array optimisation (*FLORIS* from the US National Renewable Energy Laboratory) for use in conjunction with a coastal ocean model (*Thetis*). Within this process, we test a custom greedy algorithm for micro-siting purposes. This is applied to a suite of representative idealised cases, progressing to a practical study of the Inner Sound of the Pentland Firth, UK.

2. METHODOLOGY

The shallow water equation model, Thetis[a] is combined with the analytical wake model, FLORIS[b] . FLORIS is used as a basis to perform array optimisation by importing ambient flow fields computed using Thetis, returning an optimised set of turbine coordinates. Thetis is then again used to evaluate the initial and optimised layouts, by representing the presence of turbines parameterised through momentum sink terms, allowing for an improved quantification on the impacts on flow field and overall array power. This process is demonstrated schematically in Figure 1.

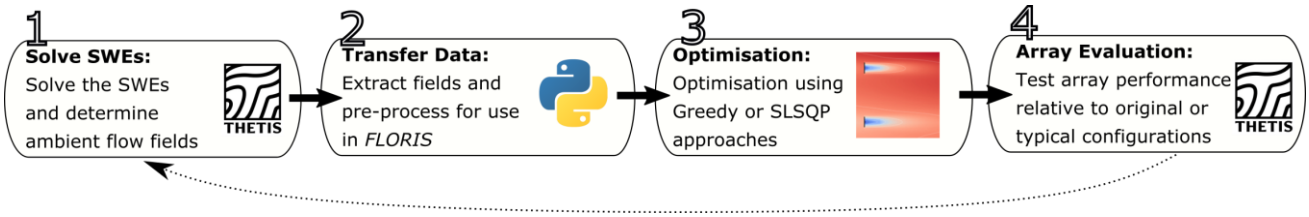

Figure 1. Schematic representation of the Thetis-Floris model combination that forms the optimisation sequence, indicating potential extensions to form an iterative process.

Shallow-water equation modelling and turbine parameterisation (*Thetis*)

Thetis is a 2-D/3-D model for coastal and estuarine flows based on the general-purpose finite element partial differential equation (PDE) solver Firedrake (Rathgeber, 2016; Karna, 2018). *Thetis* has been applied for several marine energy assessment and optimisation methods (e.g. Angeloudis et al., 2018, 2020; Mackie et al., 2021b; Goss et al., 2021). Here we consider its solver for the non-conservative form of the 2-D, depth-averaged nonlinear shallow water equations

$$\frac{\partial \eta}{\partial t} + \nabla \cdot (H_d \boldsymbol{u}) = 0, \qquad [1]$$

$$\frac{\partial \boldsymbol{u}}{\partial t} + \boldsymbol{u} \cdot \nabla \boldsymbol{u} + g\nabla\eta + f\boldsymbol{u}^{\perp} = \nabla \cdot \left(\nu(\nabla \boldsymbol{u} + \nabla \boldsymbol{u}^{T})\right) - \frac{\boldsymbol{\tau_b}}{\rho H_d} - \frac{c_t}{\rho H_d}|\boldsymbol{u}|\boldsymbol{u}, \qquad [2]$$

where η is the water elevation, $H_d = h + \eta$ is the total water depth, $\boldsymbol{u}$ is the depth-averaged velocity vector, and ν is the kinematic viscosity of the fluid. The term $f\boldsymbol{u}^{\perp}$ represents the Coriolis forcing included in non-idealised cases. In turn, $f = 2\Omega \sin(\zeta)$ with Ω the angular frequency of the Earth's rotation and ζ the latitude. In idealised cases, bed shear-stress (τ_b) effects are represented through a quadratic drag formulation, or the Manning formulation that uses the friction coefficient n_M as implemented in Vouriot et al. (2019). Finally, c_t is an additional parameterisation used to represent the turbines' thrust as a spatial field, as described in Culley et al. (2017) and Jordan et al. (2022). In particular, $c_t(\boldsymbol{x})$ is distributed within the array area using a turbine density function $d(\boldsymbol{x})$ that is prescribed based on a discrete turbine formulation, as $c_t(x) = C_t(\boldsymbol{u}(\boldsymbol{x}))A_t d(x)$,

[a] http://thetisproject.org/
[b] FLOw Redirection and Induction in Steady-state, https://floris.readthedocs.io/en/main/

thus representing the prescribed layout of the array following Funke et al. (2014). The discrete turbine formulation effectively concentrates $d(\boldsymbol{x})$ and by extension $c_t(\boldsymbol{x})$ at the turbine coordinates. The individual turbine thrust coefficient (C_t) is a function of the flow velocity and is defined based on the individual turbine characteristics, which are specified according to the representative curves of Figure 2**.** In general, the force introduced by the turbines is

$$F_{\text{array}} = \int_{\Omega_{\text{array}}} \frac{1}{2} \rho \, c_t(\boldsymbol{x}) \boldsymbol{u}(\boldsymbol{x}) \, \boldsymbol{u}(\boldsymbol{x}) \, \mathrm{d}\boldsymbol{x}. \quad [3]$$

Considering the concentration of $c_t(\boldsymbol{x})$ at the turbine coordinates, the above integral can be under-estimated, as the velocity to accurately represent the force should be the ambient velocity U_∞ upstream of the turbines rather than $\boldsymbol{u}(\boldsymbol{x})$ which within the model can be sensitive to the resistance introduced in areas where $d(\boldsymbol{x})$ is non-zero. A correction to recover the expected U_∞ is thus implemented following Kramer and Piggott (2016).

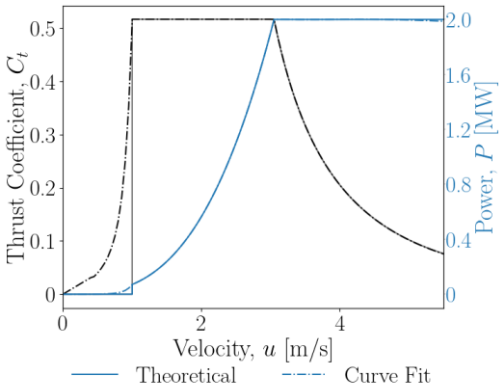

Figure 2. Thrust coefficient and Power curve considered as part of the optimisation study, based on parameters for the SIMEC Atlantis 2 MW AR2000 turbine which relates to a diameter of $D = 20$ m, capacity of 2 MW, and a rated speed (u_{rated}) of 3.05 m/s.

The shallow-water equations are discretised in the *Thetis* solver using the discontinuous Galerkin finite element method (DG-FEM) and the semi-implicit Crank-Nicolson scheme is selected for time-marching the solution. The resulting discrete system of equations is solved iteratively by Newton's method as implemented in PETSc.

2.1 Analytical wake modelling and turbine parameterisation (*FLORIS*)

In the present study, we apply FLORIS's Gaussian wake model (Bastankhah and Porte-Agel, 2014) which computes the normalised velocity deficit via the expression

$$\frac{\Delta U}{U_\infty} = \left(1 - \sqrt{1 - \frac{C_T}{8(k^* x/D + \epsilon)^2}}\right) \cdot e^{\left(-\frac{1}{2(k^* x/D+\epsilon)^2}\left\{\left(\frac{z-z_h}{D}\right)^2 + \left(\frac{y}{D}\right)^2\right\}\right)}, \quad [4]$$

Where z is the wall-normal coordinate with z_h the turbine hub height, and $k^* = k_a \cdot \mathcal{I} + k_b$ is the growth rate of the wake with coefficients k_a and k_b. $\mathcal{I}$ is the local streamwise turbulence intensity, and ϵ is the normalised Gaussian velocity deficit at the rotor plane. An important definition is the location for the onset of the far-wake (x_0), expressed as

$$x_0 = D \frac{1 + \sqrt{1 - C_t}}{\sqrt{2}\left(4\alpha \cdot \mathcal{I} + 2\beta\left(1 - \sqrt{1 - C_t}\right)\right)}, \quad [5]$$

where α, β are empirical coefficients. Wake combination is in turn implemented using the free-stream linear superposition method (Machefaux et al., 2015). Though both approaches to wake modelling are fundamentally based on the Actuator Disc Theory, there are noticeable differences between the manner in which wakes are represented in Thetis and in *FLORIS*. As such, an intermediate calibration step is required to depth-average and calibrate the analytical wakes superimposed in *FLORIS* to the ones predicted by *Thetis*

over the conditions the arrays are expected to operate. This step enables FLORIS to inform the layouts considered by the hydrodynamic model, based on the turbine characteristics of Figure 2. Our approach is to optimise a set of parameter inputs within *FLORIS*, rendering it capable to apply optimisation using the 2D flow fields from *Thetis* as flow inputs.

Table 1 Model parameters inputs

Model Parameters	**Values**
Common parameters	
Fluid density, ρ	1025 kg/m^3
Rotor swept diameter, D	20 m
Hub height, z_{hub}	18 m
Turbine cut-in speed, u_{in}	1 m/s
Turbine rated speed, u_{rated}	3.05 m/s
FLORIS-specific parameters	
Flow shear power law exponent	0
Flow veer	0
Axial induction factor (α) exponent	0.8325
Normalised downstream distance (x/d) exponent	-0.32
Initial turbulence intensity, $\mathcal{I}_0$	12%
Ambient turbulence intensity, $\mathcal{I}$	20%
Calibrated Gaussian model parameters	
k_a	0.1087
k_b	0.006912
α	0.4886
β	0.2496

2.2 Optimisation strategy

The overall objective considered is that of total energy maximisation from a tidal array system. We approach the micro-siting problem by employing an initial *Thetis* simulation of the tidal channel and extract ambient velocity fields for several instances, or *frames*, over a simulation period. Optimisation is performed in a manner that maximises the accumulated energy from each of these fields, assuming that these are representative of the established dynamics when turbines operate. If necessary, an initial (e.g. aligned/staggered) turbine layout is introduced to *FLORIS* and micro-siting is performed using an appropriate optimisation strategy subject to spatial constraints, and minimum turbine separation restrictions. *FLORIS*'s default optimisation is initially performed using the SciPy minimise function for the idealised models through the SLSQP (Sequential Least SQuares Programming) method.

Altering $2N$ variables (i.e. x-, y- coordinates for N turbines) for each flow field over 50 iterations, say, becomes highly time-consuming as the number of turbines N increases beyond a small array. An increased array size also entails a larger optimisation space, further stressing conventional optimisation, and increasing the likelihood of converging to local maxima. To address the above, a heuristic-based greedy optimisation technique is tested which positions each turbine sequentially. This allows the imposition of constraints which form acceptance criteria, sequentially adding turbines until either desired capacity is installed or no feasible positions remain. This alternative approach allows for the rejection of proposed turbine placements based on aspects such as bathymetric gradient, forming a basis for non-trivial objective functions. In this case the "greedy" algorithm iteratively identifies the maximum power of new turbine locations that satisfy spacing constraints, whilst restricting influence from the wakes of surrounding turbines. More details are presented in Jordan et al. (2022). In addition, for steady-state cases, the adjoint optimisation methodology of Funke et al. (2014) is applied for completeness.

3. CASE STUDIES

In demonstrating this tidal-array optimisation framework, we consider models of increasing complexity as in Figure 3. First, we examine the micro-siting of aligned and staggered turbine arrays in 5 row x 3 column configuration (where rows face the streamwise flow); the array itself is situated within an idealised channel of steady state flow (Case A), followed by oscillatory flow around a channel featuring a headland (Case B). For both staggered and aligned cases $2D$ lateral (between rows) spacing and $3D$ longitudinal (between columns)

spacing is imposed. (In staggered cases, this means that a $6D$ longitudinal distance between turbines on the same streamline is provided.

For our realistic flow problem (Case C) we consider the Pentland Firth region with aligned and staggered array sizes of 4x6 turbines of $5D$ lateral and longitudinal spacing, followed by a staggered 8x6 case of $3D$ spacing to extend the optimisation framework to larger arrays. The Thetis meshes that underpin these cases have been refined in within the array region to an element size of 3-5 m, subject to an unstructured mesh sensitivity analysis on wake evolution.

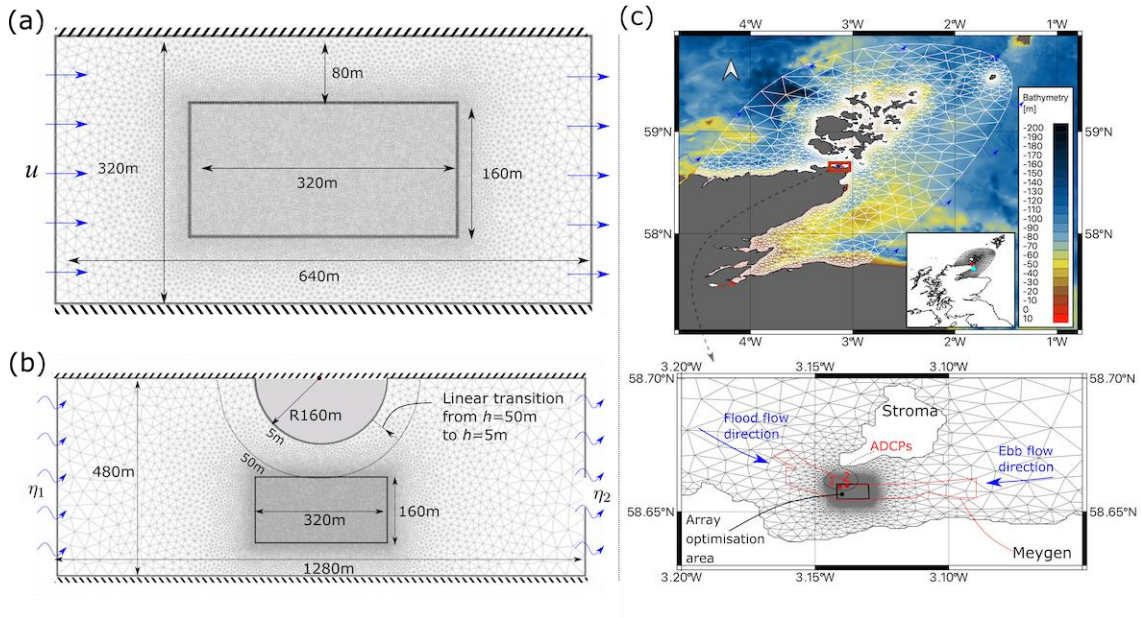

Figure 3. Case study layouts: (a) steady state rectangular channel, (b) oscillatory channel flow featuring a headland and (c) the Pentland Firth Inner Sound tidal array site.

For Case A (Figure 3a), an array site of (320 m × 160 m) provides sufficient space to position turbines across the width of the array, but it too short to prevent substantial wake recovery. Constant depth of $h = 50$ m, viscosity of $\nu_t = 1$ m^2/s and a quadratic drag coefficient of C_d= 0.0025 are imposed within the domain. Based on these parameters, steady-state conditions using an inflow velocity $u = 3.175$ m/s are imposed, with this value being close to u_{rated}. For Case B (Figure 3b), the same array size is considered off a headland which leads to localised flow acceleration due a depth transition from 50 m to 5 m along the coast. Unsteady, oscillatory flow is imposed by applying opposing sinusoidal free surface signals at the eastern and western sides of the domain of amplitude A_{tide}= 0.275 m and $T = 1$ h. Given the confined nature of the domain, a viscosity sponge of 50 m^2/s at both eastern and western boundaries is applied that linearly reduces to 1 m^2/s to ensure flow uniformity at the boundary for stability purposes.

The optimisation of arrays within the Inner Sound of the Pentland Firth is considered next (Case C, Figure 3c); this is a non-trivial case that combines complex bathymetry, asymmetric tidal flow subject to multiple tide constituents (Q1, O1, P1, K1, N2, M2, S2, K2), and significant variability of the resource within the allocated tidal array development area. The simulation has been validated to a satisfactory level using a variable Manning n_M coefficient that is based on the expected bed roughness according to records of bed sediment size distribution, as per Mackie et al. (2021), through comparisons against ADCP and tide gauge data as detailed in Jordan et al. (2022).

4. RESULTS

The results across all optimisation cases are summarised in Table 2, which lists the performance of the array once evaluated using a *Thetis* simulation that includes turbines at the prescribed coordinates. In Case A, we observe the tendency of all optimisation approaches to form fence-like structures, that maximise the distance between rows of clustered turbines, so as to avoid wake interaction effects. The fully Thetis-based adjoint optimisation performs best, by also trying to exploit blockage effects; this process is superior, but requires substantially greater computational time than alternative optimisation approaches using FLORIS. The computational time is expected to be even more cumbersome and memory-intensive in non-steady cases.

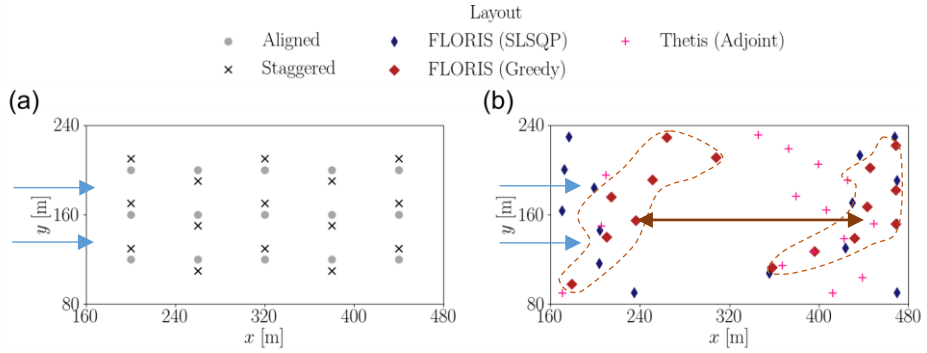

Figure 4. Array layout results for steady state case, demonstrating the tendency to structure turbines into fences, maximizing longitudinal distances in between to avoid wake interaction. Blue arrows indicate the flow direction, and the brown arrow indicates the distance between qualitatively fence-like row that emerge in the optimized layouts. The dashed orange lines identify clusters of turbines that attempt to form a column.

Table 2 Summary of optimisation cases and overall performance

#	Case	N_t	Initial Layout	Optimisation Approach	L_{min}	N_{frames}	Average Power |P| [MW]	Optimisation time[f] t_{opt} [min]
A.1	**Channel**[c]	15	Aligned	-	2*D*	-	**25.00**	-
A.2	**Channel**	15	Staggered	-	2*D*	-	28.97 (+15.9%)	-
A.3	**Channel**	15	Aligned	FLORIS (SLSQP)	1.5*D*	1	29.81 (+19.2%)	4.1
A.4	**Channel**	15	-	FLORIS (Greedy)	1.5*D*	1	29.22 (+16.9%)	3.3
A.5	**Channel**	15	Aligned	Thetis-Adjoint (SLSQP)	1.5*D*	N/A	29.96 (+19.8%)	197.1
B.1	**Headland**[d]	15	Aligned	-	2*D*	-	**7.82**	-
B.2	**Headland**	15	Staggered	-	2*D*	-	8.83 (+12.8%)	-
B.3	**Headland**	15	Aligned	FLORIS (SLSQP)	1.5*D*	6	10.06 (+28.6%)	361.9
B.4	**Headland**	15	-	FLORIS (Greedy)	1.5*D*	6	9.56 (+22.3%)	7.8
C.1	**Pentland Firth**[e]	24	Aligned	-	5*D*	-	**20.47**	-
C.2	**Pentland Firth**	24	Staggered	-	5*D*	-	20.55 (+0.4%)	-
C.3	**Pentland Firth**	24	Aligned	FLORIS (SLSQP)	3*D*	18	21.72 (+6.1%)	4002
C.4	**Pentland Firth**	24	-	FLORIS (Greedy)	3*D*	18	23.01 (+12.4%)	0.8
C.5	**Pentland Firth**	24	-	FLORIS (Greedy)	1.5*D*	18	23.71 (+15.8%)	2.8
C.6	**Pentland Firth**	48	Staggered	-	3*D*	-	**40.33**	-
C.7	**Pentland Firth**	48	-	FLORIS (Greedy)	1.5*D*	18	42.43 (+5.2%)	12.1

In Case B, similar trends are observed, with turbine rows positioned to face ebb and flood flows, whilst turbines are placed in a staggered manner to avoid wake interactions (Figure 5). In this case the gradient-based SLSQP approach (B.3, Table 2), delivers the best results through an improvement of 28.6%, but is remarkably prone to exploring poor local maxima, and requires a substantially amount of time when applying the wake superposition process over multiple number of frames (N_{frames}). The greedy approach delivers a notable (+22.3%) improvement to the original aligned/ staggered layouts at a reduced optimisation time.

[c] All optimisation simulations were run on a single core. Specification: Intel (R) Xeon (R) Gold 5118 CPU @ 2.30GHz.
[d] Thetis run for 39.3 min of time on 1 core for confirmed convergence to steady state (3.5 hour simulation time).
[e] Thetis run time of 27.4 min on 4 cores, for 8 hours simulation time.
[f] Thetis run time of 1337.1 min on 12 cores, for a 30 day simulation time.

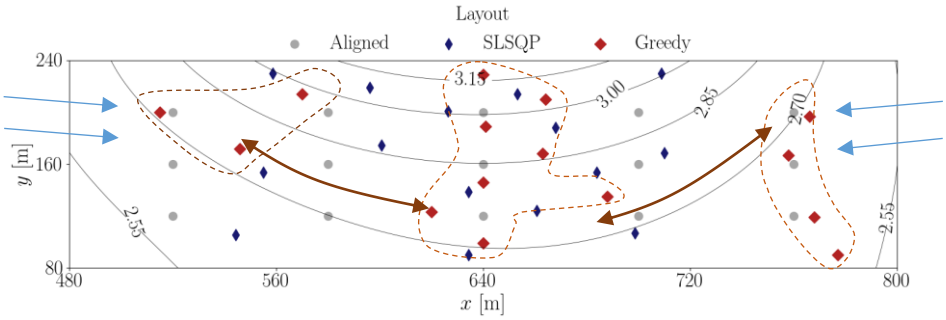

Figure 5. Array optimisation layout results for transient case study of oscillatory flow around an idealised channel featuring a headland. Similar trends are observed to the steady case, with an attempt to position fences to face both tidal flow directions. Blue arrows indicate the flow direction, and the brown arrow indicates the distance between qualitatively fence-like row that emerge in the optimized layouts. The dashed orange lines identify clusters of turbines that attempt to form a column, while the grey contours correspond to the velocity amplitude of the tidal signal.

In the more complex case considering a tidal array in the Inner sound of the Pentland Firth, the greedy optimisation case performs best, with the heuristic approach identifying and prioritising the high power density areas (Figure 6). The optimisation appears to be most efficient during neap conditions, as turbines operate below their rated capacity, and their power generation is thus more vulnerable to wake interactions. The benefit of the optimisation seems to reduce when more dense turbine array configurations are considered (C.7), where a more noticeable array feedback is observed through array blockage. Effectively due to additional resistance by the presence of the array, the volume flux change ($\Delta Q/Q_{\mathrm{amb}}$) increases from ~3.5% to ~7.7%, when transitioning from 24 to 48 turbines, indicating the onset of noticeable effects through array blockage. In terms of global blockage, for 24 turbines the volume flux through the inner sound peaks by ~-0.6% in the cases of 24 turbines, with this reduction increasing to ~-1.2% through the installation of 48 turbines.

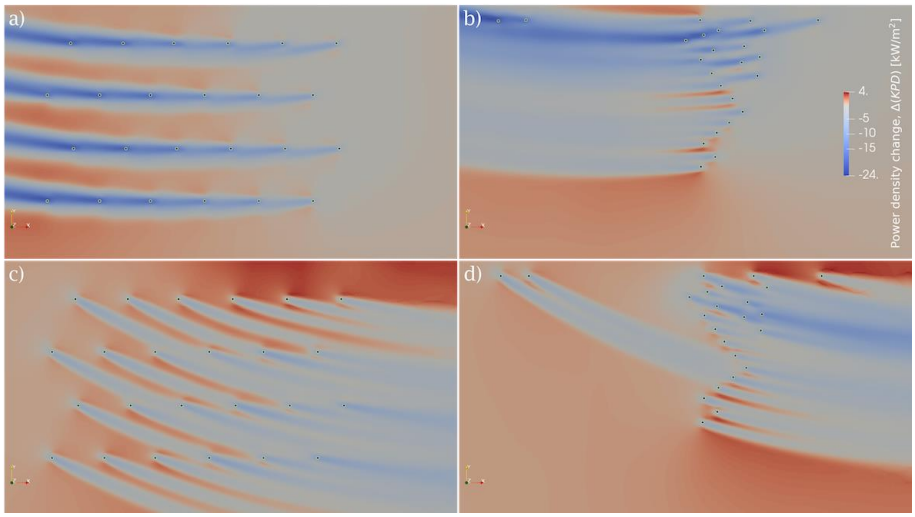

Figure 6 Power density changes due to different turbine configurations for the Pentland Firth case study over spring tide flow. Turbines are positioned in regions of higher power density, with turbines sometimes positioned in the wake of upstream turbines if flow speeds are predominantly above u_{rated}.

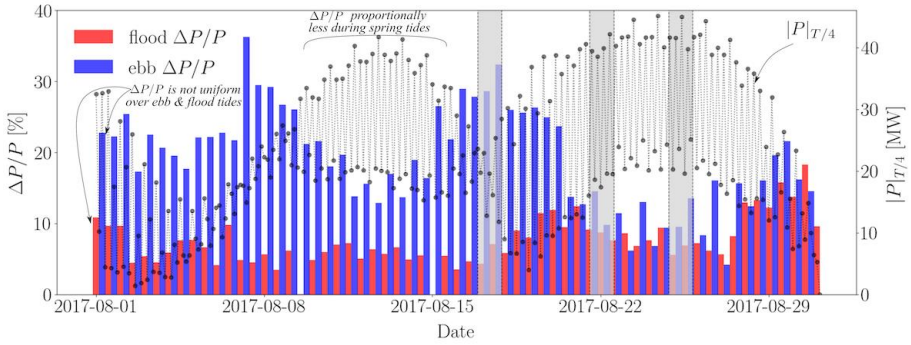

Figure 7 Proportional increase of power output relative to original turbine array configuration over a 30 day period.

5. DISCUSSION

The general array micro-siting pattern returned by the optimisation approaches (SLSQP and greedy alike) sees turbines positioned within high power density regions and otherwise spread to maintain separation whilst avoiding wake interaction. This also agrees with results reported previously Stansby and Stallard (2016) that emphasise wake avoidance within the optimisation process. Under operational conditions below u_{rated}, variation in wake representation can compromise optimisation, as key velocity deficit areas may not be captured accurately. If the wake width is underestimated in the analytical model, then some of the turbines may become partially immersed in upstream wakes when evaluated by the hydrodynamic model. This highlights the significance of calibrating the wake model parameters. Additional parameters can be considered to improve accuracy, such as varying the turbulent intensity, I, as a function of the flow magnitude, for better agreement against data. These were assumed constant in this study for simplicity but should be calibrated accordingly as they are subject to inflow conditions and varying turbulence levels. The further inclusion of local blockage effects, which has been shown to be possible through ad-hoc corrections in analytical approaches such as *FLORIS* (Branlard et al., 2020), could also benefit optimisation in high-density, confined scenarios. Otherwise, the application of optimisation within sections of the array in an iterative manner (as in **Figure 1**), could provide an avenue to allow the hydrodynamic model to inform about the array hydrodynamic impacts whilst constraining the number of variables (e.g. number of turbines and domain size) which can act as bottlenecks in the optimisation problem.

The optimisation approach described here relies on the use of analytical wake models that typically assume steady-state conditions. The practice of wake superposition itself introduces a mass and momentum deficit; these necessitate the assessment of *FLORIS*-derived layouts within hydrodynamics models. On the other hand, the hydrodynamics model (in this case *Thetis*) does not capture horizontal flow structures below the mesh-size scale which means that many unsteady and quasi-steady flow phenomena are not considered in our analysis. This may have implications for the final prediction of the wake deficits and therefore also affect the optimal array layout solution. One phenomenon of relevance which is not captured in our simulations is dynamic wake meandering. As turbine wakes interact with the larger tidal-channel turbulent structures, such as near-wall high- and low-speed streaks, near-wake vortices start breaking down giving way to the generation of a cascade of turbulent scales. Additionally, the wake experiences lateral and vertical displacements caused by the larger-scales leading to their significant lateral expansion. These effects are not encapsulated within hydrodynamic models unless the model spatial and temporal resolution is increased and/or combined with more robust turbulence models that capture these effects while avoiding excessive dissipation in the solution. Inherently, all 2-D models are limited in their ability to capture dispersion effects due to the assumed uniform vertical velocity. 3-D shallow-water models on the other hand, can improve the representation of such scales through the addition of a horizontal mixing length scale (Stansby, 2003) which alters the velocity profile over the water column, resulting in greater vertical shear; however, further research is required in order to quantify their impact on wake dynamics.

6. CONCLUSION

A novel optimisation method was demonstrated by retrofitting an analytical wake superposition model, in this case *FLORIS*, for use with a coastal hydrodynamics model, *Thetis*. The method is motivated upon reflection on the bottlenecks observed in existing array optimisation approaches, which depending on acceptable computational costs may be constrained to (a) simplified flow geometries, (b) steady-state flow conditions and (c) idealised turbine representations. The methodology was applied to three cases of

increasing complexity (in terms of geometry, oscillatory flow, and array turbine number), demonstrating its potential to deliver substantially improved tidal array layouts. In particular, the optimisation scenario of 24 turbines in a confined region within the Pentland Firth demonstrated the ineffectiveness of staggered arrangements for non-rectilinear oscillatory flows, and the computationally efficient application of this methodology for complex geometries and flow dynamics. It was found that the resultant method yielded an overall improvement in power output in the order of 12% for 3*D* minimum spacing and up to almost 16% when reduced to 1.5*D*. Finally, it was observed that flow asymmetry in conjunction with minimum distance requirements may render the exploitation of local blockage effects rather challenging. Case studies using 24 and then 48 turbines respectively within the Meygen site at the Pentland Firth indicated low levels of global blockage. However, as the number of turbines doubles to 48 in the latter case, blockage effects start to become more noticeable. Given the extensions expected as tidal arrays expand, it is proposed that the optimisation approach presented can be operated iteratively enabling the hydrodynamic model to account for array-scale blockage as the size of the array is extended.

7. ACKNOWLEDGEMENTS

A. Angeloudis acknowledges the support of the NERC Industrial Innovation fellowship grant NE/R013209/2 and the support of the EC H2020 ILIAD DTO project under grant agreement 101037643. D. Coles acknowledges the support of the Tidal Stream Industry Energiser project (TIGER), co-financed by the European Regional Development Fund through the INTERREG France (Channel) England Programme. M. Piggott acknowledges the support of EPSRC under grants EP/M011054/1 and EP/R029423/1.

8. REFERENCES

Angeloudis, A., Kramer, S. C., Avdis, A., & Piggott, M. D. (2018). Optimising tidal range power plant operation. *Applied energy*, *212*, 680-690.

Angeloudis, A., Kramer, S. C., Hawkins, N., & Piggott, M. D. (2020). On the potential of linked-basin tidal power plants: An operational and coastal modelling assessment. *Renewable Energy*, *155*, 876-888.

Bastankhah, M., & Porté-Agel, F. (2014). A new analytical model for wind-turbine wakes. *Renewable Energy*, *70*, 116–123. https://doi.org/10.1016/j.renene.2014.01.002

Branlard, E., & Meyer Forsting, A. R. (2020). Assessing the blockage effect of wind turbines and wind farms using an analytical vortex model. *Wind Energy*, *23*(11), 2068–2086. https://doi.org/10.1002/we.2546

Coles, D., Angeloudis, A., Greaves, D., Hastie, G., Lewis, M., Mackie, L., McNaughton, J., Miles, J., Neill, S., Piggott, M., Risch, D., Scott, B., Sparling, C., Stallard, T., Thies, P., Walker, S., White, D., Willden, R., & Williamson, B. (2021). A review of the UK and British Channel Islands practical tidal stream energy resource. Proceedings of the Royal Society A: Mathematical, Physical and Engineering Sciences, 477(2255), 20210469. https://doi.org/10.1098/rspa.2021.0469

Culley, D. M., Funke, S. W., Kramer, S. C., & Piggott, M. D. (2016). Integration of cost modelling within the micro-siting design optimisation of tidal turbine arrays. *Renew. Energy*, *85*, 215–227. https://doi.org/10.1016/j.renene.2015.06.013

Divett, T., Vennell, R., & Stevens, C. (2016). Channel-scale optimisation and tuning of large tidal turbine arrays using LES with adaptive mesh. *Renewable Energy*, *86*, 1394–1405. https://doi.org/10.1016/j.renene.2015.09.048

Funke, S. W., Farrell, P. E., & Piggott, M. D. (2014). Tidal turbine array optimisation using the adjoint approach. Renewable Energy, 63, 658–673. https://doi.org/10.1016/j.renene.2013.09.031

Goss, Z. L., Coles, D. S., Kramer, S. C., & Piggott, M. D. (2021). Efficient economic optimisation of large-scale tidal stream arrays. *Applied Energy*, *295*, 116975.

Jordan, C., Dundovic, D., Fragkou, A., Deskos, G., Coles, D., Piggott, M. D., & Angeloudis, A., (2022). Combining shallow-water and analytical wake models for tidal array micro-siting, *Journal of Ocean Engineering and Marine Energy* (Accepted).

Kärnä, T., Kramer, S. C., Mitchell, L., Ham, D. A., Piggott, M. D., & Baptista, A. M. (2018). Thetis coastal ocean model: discontinuous Galerkin discretization for the three-dimensional hydrostatic equations. *Geoscientific Model Development Discussions*, *2018*, 1–36. https://doi.org/10.5194/gmd-2017-292

Kramer, S. C., & Piggott, M. D. (2016). A correction to the enhanced bottom drag parameterisation of tidal turbines. *Renewable Energy*, *92*, 385–396. https://doi.org/10.1016/j.renene.2016.02.022

Machefaux, E., Larsen, G. C., & Leon, J. P. M. (2015). Engineering models for merging wakes in wind farm optimization applications. *Journal of Physics: Conference Series*, *625*(1). https://doi.org/10.1088/1742-6596/625/1/012037

Mackie, L., Evans, P. S., Harrold, M. J., O`Doherty, T., Piggott, M. D., & Angeloudis, A. (2021). Modelling an energetic tidal strait: investigating implications of common numerical configuration choices. *Applied Ocean Research*, *108*(January), 102494. https://doi.org/10.1016/j.apor.2020.102494.

Mackie, L., Kramer, S. C., Piggott, M. D., & Angeloudis, A. (2021b). Assessing impacts of tidal power lagoons of a consistent design. Ocean Engineering, 240, 109879.

Neill, S. P., Haas, K. A., Thiébot, J., & Yang, Z. (2021). A review of tidal energy—Resource, feedbacks, and environmental interactions. Journal of Renewable and Sustainable Energy, 13(6), 62702. https://doi.org/10.1063/5.0069452

Phoenix, A., & Nash, S. (2019). Optimisation of tidal turbine array layouts whilst limiting their hydro-environmental impact. *Journal of Ocean Engineering and Marine Energy*, *5*(3), 251–266. https://doi.org/10.1007/s40722-019-00145-8

Piggott, M. D., Kramer, S. C., Funke, S. W., Culley, D. M., & Angeloudis, A. (2021). Optimization of Marine Renewable Energy Systems. In *Comprehensive Renewable Energy, 2nd Edition*. Elsevier. https://doi.org/https://doi.org/10.1016/B978-0-12-819727-1.00179-5

Rathgeber, F., Ham, D. A., Mitchell, L., Lange, M., Luporini, F., Mcrae, A. T. T., Bercea, G.-T., Markall, G. R., & Kelly, P. H. J. (2016). Firedrake: Automating the Finite Element Method by Composing Abstractions. *ACM Trans. Math. Softw.*, *43*(3), 24:1-24:27. https://doi.org/10.1145/2998441.

Stansby, P. K. (2003). A mixing-length model for shallow turbulent wakes. *Journal of Fluid Mechanics*, *495*, 369–384. https://doi.org/10.1017/S0022112003006384

Stansby, P., & Stallard, T. (2016). Fast optimisation of tidal stream turbine positions for power generation in small arrays with low blockage based on superposition of self-similar far-wake velocity deficit profiles. *Renewable Energy*, *92*, 366–375. https://doi.org/10.1016/j.renene.2016.02.019

Vouriot, C. V. M., Angeloudis, A., Kramer, S. C., & Piggott, M. D. (2019). Fate of large-scale vortices in idealized tidal lagoons. *Environmental Fluid Mechanics*. https://doi.org/10.1007/s10652-018-9626-4.

Zhang, J., Zhang, C., Angeloudis, A., Kramer, S. C., He, R., & Piggott, M. D. (2022). Interactions between tidal stream turbine arrays and their hydrodynamic impact around Zhoushan Island, China. *Ocean Engineering*, *246*, 110431. https://doi.org/10.1016/J.OCEANENG.2021.110431

